

Unitary meson-exchange calculation of $NN \rightarrow NN\pi$ reaction

A. Matsuyama*

*Swiss Institute for Nuclear Research, Villigen, Switzerland
and TRIUMF, Vancouver, British Columbia, Canada V6T 2A3*

T.-S. H. Lee

Physics Division, Argonne National Laboratory, Argonne, Illinois 60439

(Received 19 May 1986)

Within a unitary πNN theory a set of coupled integral equations have been developed for the study of pion production from NN collisions, and have been applied to calculate the coincidence cross sections of $pp \rightarrow pn\pi^+$ at 800 MeV. The calculation is based on a meson-exchange Hamiltonian which was previously constructed to describe NN elastic scattering up to 1 GeV by extending the Paris potential to include Δ excitation. It involves solving a Faddeev-Alt-Grassberger-Sandhas scattering equation for the final πNN state and a $NN \leftrightarrow N\Delta$ coupled-channel equation for the initial NN state. We present the procedure of using the newly developed spline function method to solve the considered Faddeev-Alt-Grassberger-Sandhas equation directly on the real momentum axis. The importance of using a unitary approach to treat the initial NN and final πNN scattering is analyzed in detail, in order to understand the results obtained in several previous approaches by Betz, Dubach *et al.*, and Verwest. The calculated cross sections reproduce the main features of the data both in magnitude and shape. The main difficulty of the present theory is found to be in reproducing the polarization data A_y . Our results provide further evidence that the πNN dynamics cannot be described completely by the conventional meson-exchange model.

I. INTRODUCTION

Extensive data¹⁻⁵ on pion production from nucleon-nucleon (NN) collisions have become available in the past few years. The study of these data is clearly an important step in the investigation of the basic mechanisms of the coupled $NN + \pi NN$ system. In this paper we report such a study within a unitary πNN formulation which has been recently developed by us.⁶ The essential point of our approach is to formulate a unitary πNN scattering theory which can describe both the conventional meson-exchange mechanisms and the possible dibaryonic excitations of (one-body) six-quark states. The application of our theory can be carried out in practice by using computation methods developed in the coupled-channel NN calculation⁷ and the Faddeev-Alt-Grassberger-Sandhas (AGS) πd calculation.⁸ This has been demonstrated in a recent paper⁹ in which we show how these two works are combined to carry out a unitary calculation of both NN and πd elastic scattering, using *nonseparable* meson-exchange models of baryon-baryon interactions. In this paper we show that a similar extension will allow us to carry out a unitary calculation of $NN \rightarrow NN\pi$ reaction. Our objective is to continue our efforts in Refs. 7 and 9 to rigorously explore the extent to which the πNN reactions can be described by the conventional meson-exchange models. As discussed in Ref. 6, this is a necessary task for investigating the genuine six-quark dynamics.

As a first step, we focus our attention in this paper on the Δ -excitation mechanism. We therefore will study the $NN \rightarrow NN\pi$ reaction based on the model Hamiltonian developed in Refs. 7 and 9. It takes the following form,

$$H = H_0 + V_{NN,NN} + h_{\pi N \leftrightarrow \Delta} + V_{NN \leftrightarrow N\Delta}, \quad (1.1)$$

where H_0 is the free energy operator, and $V_{NN,NN}$ is a NN potential. The pion production mechanism $NN \rightarrow N\Delta \rightarrow NN\pi$ is clearly due to the last two transition operators, $h_{\pi N \leftrightarrow \Delta}$ and $V_{NN \leftrightarrow N\Delta}$. In this Hamiltonian formulation, the pion and Δ degrees of freedom also influence the NN scattering at energies below the pion production threshold. Therefore, the potential $V_{NN,NN}$ in Eq. (1.1) cannot be identified with a conventional low energy NN potential. In Ref. 7 a subtraction procedure is introduced to define $V_{NN,NN}$ from the Paris potential.¹⁰ The only freedom in using this procedure to construct the πNN model equation (1.1) is in the parametrization of the $NN \leftrightarrow N\Delta$ transition potential. It has been found^{7,9} that the NN phase shifts as well as various total cross sections up to about 1 GeV can be described to a very large extent if $V_{NN \leftrightarrow N\Delta}$ is parametrized as the sum of pion and rho exchange with the cutoff parameter¹¹ of its dipole form factor chosen to be $\Lambda = 650$ MeV/c. Our results as well as the construction procedure can be found in Refs. 7 and 9 and will not be repeated here. We only want to emphasize here that *the present $NN \rightarrow NN\pi$ study is based on the same model, and hence does not involve any adjustable parameter.*

With this well-defined model Hamiltonian equation (1.1), it is clear that there are two different pion production processes, as illustrated in Fig. 1. The first one [Fig. 1(a)] will be called the direct Δ -production process, while the second [Fig. 1(b)] will be called the final state interaction (FSI) process. Their precise meaning will become clear in Sec. II. The production strength is clearly deter-

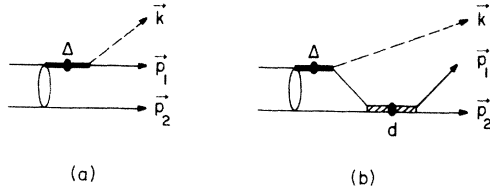


FIG. 1. The $NN \rightarrow NN\pi$ reaction mechanisms which can be generated from the model Hamiltonian equation (1.1). (a) The direct Δ production process; (b) the final state interaction (FSI) process.

mined by the dynamical content of the initial $NN \rightarrow N\Delta$ transition matrix. In the unitary πNN approach of this work, it contains all possible $NN \rightarrow N\Delta$ transitions which can be generated, in the subspace $NN \oplus N\Delta \oplus \pi NN$, from all interaction terms of Eq. (1.1). We will show in this work that the amplitudes of these two processes can be calculated from the solutions of a set of coupled integral equations deduced from the general unitary πNN formulation of Ref. 6.

Equation (1.1) is also the basis of an early meson-exchange calculation by Betz.¹² The main differences between his calculation and the present work are in the parametrization of the baryon-baryon interactions and the treatment of the πNN unitary cut. Although Betz was able to get a reasonable description of the $NN \rightarrow NN\pi$ cross section by adjusting the parameters of the one-boson-exchange model of baryon-baryon interactions, he did not show that the same set of parameters also gives a good description of NN and πd elastic scattering. We will see in Sec. II that our $NN \rightarrow NN\pi$ calculation is consistent with our previous calculations of NN and πd elastic scattering, as is required by the πNN unitarity condition. The calculation by Betz neglected the πNN final state interaction [Fig. 1(b)]. In calculating the initial $NN \rightarrow N\Delta$ transition, he also neglected the effect due to the one-pion-exchange $N\Delta \rightarrow \Delta N$ interaction induced by the vertex interaction $h_{\pi N \leftrightarrow \Delta}$. We do not make these two approximations.

Based on a different unitary formulation of the problem, the $NN \rightarrow NN\pi$ reaction has also been studied by Dubach, Kloet, Cass, and Silbar.^{13,14} The dynamical content of their calculations is essentially the one-pion-exchange (OPE) model of Kloet and Silbar.¹⁵ Their approach, therefore, contains the same theoretical uncertainty as Betz's calculation, since it can be seen from Ref. 15 that the OPE model does not satisfactorily describe the NN elastic scattering. By examining the OPE limit of our theory, we will try to assess, at least qualitatively, their results from a more dynamical point of view.

Another existing approach to the study of the $NN \rightarrow \pi NN$ reaction is based on the lowest order Feynman diagram in the one-boson-exchange approximation. For instance, the early work by Verwest¹⁶ was done by adjusting the parameters of the baryon-baryon-meson form factors to fit the production data directly. From the point of view of exploring the basic πNN dynamics, the significance of these fitted parameters are not clear since they

also contain distortion effects due to the initial NN and final πNN scattering. We will demonstrate that because of the strong initial NN and final πNN distortions, a direct interpretation of the $NN \rightarrow NN\pi$ data, especially the polarization observables, in terms of the lowest order one-boson-exchange mechanism, is not very meaningful.

Apart from having a more consistent and richer dynamical input than all of the previous approaches, an important feature of our approach is a Faddeev-AGS treatment⁸ of the πNN final state interaction illustrated in Fig. 1(b). As is well known in the literature,¹⁷ it is a non-trivial numerical problem to treat a three-body final state interaction (FSI). We overcome this problem by using a new numerical method¹⁸ developed in a study of πd breakup reactions to handle the πNN branch cut. Our rigorous treatment of FSI will provide information for assessing the simple phenomenological parametrization of FSI used in Refs. 14 and 16 and in most existing studies of pion production processes.

In Sec. II we recall the formulation of Ref. 6 to derive the πNN scattering equations for the calculation of the $NN \rightarrow NN\pi$ reaction in the Δ -excitation region. In Sec. III the numerical methods used in our calculation will be briefly described. We discuss our results in Sec. IV. Section V is devoted to summarizing our approach and discussing future improvements.

II. UNITARY πNN SCATTERING EQUATION

The basic idea of our unitary formulation in Ref. 6 is to separate the $\pi(\Delta)$ multiple scattering mechanism from the rest of the πNN dynamics. While the multiple scattering can be treated by the well-developed Faddeev-AGS method,⁸ the effect of the essential meson-exchange baryon-baryon (nonseparable) interaction is rigorously calculated by using the coupled-channel method developed in the study of NN scattering.^{7,9} The formalism needed for the present study in the Δ resonance energy region can be obtained from Sec. III of Ref. 6 by omitting the non-resonant interactions $v_{\pi N}$ and $F_{\pi NN \leftrightarrow NN}$. In this special case the πNN Hamiltonian is reduced to the form of Eq. (1.1) and the amplitude for pion production in NN collisions is defined by only the first term of Eq. (3.69) of Ref. 6. It can be cast into the following form,

$$T_{\pi NN, NN} = T_{\pi NN, N\Delta}^F \frac{P_{N\Delta}}{E - H_0} T_{N\Delta, NN}, \quad (2.1)$$

where $P_{N\Delta}$ is the projection operator for the $N\Delta$ state and H_0 is the free Hamiltonian. The $NN \rightarrow N\Delta$ transition operator is defined by

$$T_{N\Delta, NN}(E) = V_{N\Delta, NN} \Omega_{NN}^{(+)}(E), \quad (2.2a)$$

with

$$\Omega_{NN}^{(+)}(E) = 1 + \frac{P_{NN}}{E - H_0} T_{NN, NN}(E), \quad (2.2b)$$

where $V_{N\Delta, NN}$ is the $N\Delta \leftrightarrow NN$ transition potential and

$T_{NN,NN}$ is the NN elastic scattering operator. Equation (2.2) indicates that the NN elastic scattering is an important ingredient of the pion production calculation. The elastic amplitude is, of course, also influenced by the pion

production channel. This has been formulated in Sec. III A of Ref. 6. For the Δ -excitation model considered in this work, the elastic scattering operator is defined by the following equations (see also Ref. 9):

$$T_{NN,NN}(E) = [V_{NN,NN} + \mathcal{V}_{NN,NN}(E)] \left[1 + \frac{P_{NN}}{E - H_0} T_{NN,NN}(E) \right], \quad (2.3a)$$

with

$$\mathcal{V}_{NN,NN}(E) = V_{NN,N\Delta} \frac{P_{N\Delta}}{E - H_0 - \Sigma_{\Delta}(E)} \left[1 + X_{N\Delta,N\Delta}(E) \frac{P_{N\Delta}}{E - H_0 - \Sigma_{\Delta}(E)} \right] V_{N\Delta,NN}. \quad (2.3b)$$

The effect of the pion production mechanism is contained in $\mathcal{V}_{NN,NN}(E)$, in which the AGS amplitude $X_{N\Delta,N\Delta}$ will be defined later. $\Sigma_{\Delta}(E)$ is the Δ self-energy calculated from the $\pi N \leftrightarrow \Delta$ vertex. The construction of $V_{NN,NN}$ from the Paris potential as well as the method of solving Eq. (2.3) have been discussed in Refs. 7 and 9.

The multiple scattering amplitude $T_{\pi NN,N\Delta}^F$ is defined by Eq. (3.42) of Ref. 6. When the nonresonant πN interactions are neglected, it takes the following form:

$$T_{\pi NN,N\Delta}^F(E) = \left\langle \pi NN \left| V^F + V^F \frac{1}{E - H_0 - V^F} V^F \right| N\Delta \right\rangle, \quad (2.4a)$$

with

$$V^F = h_{\pi N \leftrightarrow \Delta} + V_{NN,NN}. \quad (2.4b)$$

By using the following well-known operator relation

$$\frac{1}{A - B} = \frac{1}{A} + \frac{1}{A - B} B \frac{1}{A},$$

it is easy to see that

$$T_{\pi NN,N\Delta}^F \frac{P_{N\Delta}}{E - H_0} = \left\langle \pi NN \left| \left[V^F + V^F \frac{1}{E - H_0 - V^F} V^F \right] \frac{1}{E - H_0} \right| N\Delta \right\rangle P_{N\Delta} = \left\langle \pi NN \left| V^F \frac{1}{E - H_0 - V^F} \right| N\Delta \right\rangle P_{N\Delta}. \quad (2.5)$$

We now follow the standard AGS method to calculate Eq. (2.5). The simplicity comes from the use of approximation that the NN scattering *in the presence of a spectator pion* can be calculated from the following separable representation of $V_{NN,NN}$,

$$V_{NN,NN} = |v_d\rangle \langle v_d|, \quad (2.6)$$

where d denotes all of the quantum numbers needed to specify the quasiparticle in the AGS approach. Note that the separable representation equation (2.6) is only used in solving Eq. (2.5), but not in the NN calculation equation (2.3). The $\pi N \leftrightarrow \Delta$ vertex interaction can also be written as a separable form,

$$h_{\pi N \leftrightarrow \Delta} = |h_{\pi N, \Delta}\rangle \langle \Delta| + |\Delta\rangle \langle h_{\pi N, \Delta}|. \quad (2.7)$$

Substituting the separable interactions equations (2.6) and (2.7) into Eq. (2.5), it is straightforward to show that

$$T_{\pi NN,N\Delta}^F \frac{P_{N\Delta}}{E - H_0} = h_{\pi N, \Delta} [1 + G_{N\Delta}(E) X_{N\Delta,N\Delta}(E)] G_{N\Delta}(E) + v_d G_{\pi d}(E) X_{\pi d, N\Delta}(E) G_{N\Delta}(E), \quad (2.8)$$

where $G_{N\Delta}$ and $G_{\pi d}$ are the propagators dressed respectively by $h_{\pi N, \Delta}$ and v_d in the well-known way.⁸ The AGS amplitudes are defined by the following coupled integral equations,

$$X_{N\Delta,N\Delta}(E) = Z_{N\Delta,N\Delta}(E) [1 + G_{N\Delta}(E) X_{N\Delta,N\Delta}(E)] + Z_{N\Delta,\pi d}(E) G_{\pi d}(E) X_{\pi d, N\Delta}(E) \quad (2.9a)$$

$$X_{\pi d, N\Delta}(E) = Z_{\pi d, N\Delta} + Z_{\pi d, N\Delta}(E) G_{N\Delta}(E) X_{N\Delta,N\Delta}(E), \quad (2.9b)$$

where $Z_{N\Delta,N\Delta}$ and $Z_{N\Delta,\pi d}$ are, respectively, the π - and N -exchange interaction⁸ in a subspace spanned by “two-body” πd and $N\Delta$ states. Note that $X_{N\Delta,N\Delta}$ is also the input to the πNN interaction term $\mathcal{V}_{NN,NN}$ of Eq. (2.3b) for NN elastic scattering calculations, if the same separable approximation equation (2.6) is used to calculate the “connected” $N\Delta$ scattering term T_c defined by Eqs. (5) and (6) of Ref. 9. In the standard partial-wave representation, the above equations reduce to one-dimensional coupled integral equations and can be handled with the existing computation power. The use of this AGS approximation is, of course, justified by its success in giving a reasonable description of πd elastic scattering.⁸

Substituting Eq. (2.8) into Eq. (2.1), we have

$$T_{\pi NN, NN}(E) = h_{\pi N, \Delta} G_{N\Delta}(E) X_{N\Delta, NN}(E) + v_d G_{\pi d}(E) X_{\pi d, NN}(E), \quad (2.10)$$

where

$$X_{N\Delta, NN}(E) = [1 + X_{N\Delta, N\Delta}(E) G_{N\Delta}(E)] T_{N\Delta, NN}(E), \quad (2.11a)$$

$$X_{\pi d, NN}(E) = X_{\pi d, N\Delta}(E) G_{N\Delta}(E) T_{N\Delta, NN}(E). \quad (2.11b)$$

The meanings of the direct Δ -production [Fig. 1(a)] and the FSI process [Fig. 1(b)] are now precisely defined by the first and second terms of Eq. (2.10), respectively. By using AGS equation (2.9), it is easy to cast Eq. (2.11) into

$$X_{N\Delta, NN}(E) = T_{N\Delta, NN}(E) + Z_{N\Delta, N\Delta}(E) G_{N\Delta}(E) X_{N\Delta, NN}(E) + Z_{N\Delta, \pi d}(E) G_{\pi d}(E) X_{\pi d, NN}(E), \quad (2.12a)$$

$$X_{\pi d, NN}(E) = Z_{\pi d, N\Delta}(E) G_{N\Delta}(E) X_{N\Delta, NN}(E). \quad (2.12b)$$

Equation (2.12) is graphically illustrated in Fig. 2. The main feature of the above equations is that the driving term $T_{N\Delta, NN}$ contains the crucial meson-exchange and short-range mechanisms which have been well tested in the study of NN scattering.^{7,9} As discussed in Sec. I, this is the key difference between our approach and all of the previous approaches. For our latter discussions, we note that Eq. (2.12) can be exactly cast into the familiar distorted form

$$X_{N\Delta, NN}(E) = \Omega_{N\Delta}^{(-)+}(E) V_{N\Delta, NN} \Omega_{NN}^{(+)}(E), \quad (2.13a)$$

$$X_{\pi d, NN}(E) = \Omega_{\pi d}^{(-)+}(E) V_{N\Delta, NN} \Omega_{NN}^{(+)}(E), \quad (2.13b)$$

where $\Omega_{NN}^{(+)}$ has been defined by Eq. (2.2b). The distortion operators for $N\Delta$ and πd are defined by

$$X_{N\Delta, NN}^{JP}(p, p_0) = T_{N\Delta, NN}^{JP}(p, p_0) + \int p'^2 dp' Z_{N\Delta, N\Delta}^{JP}(p, p') G_{N\Delta}(p') X_{N\Delta, NN}^{JP}(p', p_0) + \int p'^2 dp' Z_{N\Delta, \pi d}^{JP}(p, p') G_{\pi d}(p') X_{\pi d, NN}^{JP}(p', p_0), \quad (3.1a)$$

$$X_{\pi d, NN}^{JP}(p, p_0) = \int p'^2 dp' Z_{\pi d, N\Delta}^{JP}(p, p') G_{N\Delta}(p') X_{N\Delta, NN}^{JP}(p', p_0). \quad (3.1b)$$

Here the notations NN, $N\Delta$, and πd now stand for the necessary quantum numbers for each channel with total angular momentum J and parity P , and p_0 is the initial on-shell NN relative momentum. The difficulty of solving Eq. (3.1) is due to the πNN three-body cut which results in a logarithmic singularity in the driving terms Z . This can be handled by the standard contour rotation method¹⁹ if the analytic structure of the other driving term $T_{N\Delta, NN}$ is also known. However, this is difficult to do in practice since in the considered meson-exchange model, Eq. (1.1) based on the Paris potential, it is not easy to determine the analytic structure of $T_{NN, NN}$ and hence also $T_{N\Delta, NN}$. For this reason we need to depart from conventional practice and use a different numerical method for solving the integral equation (3.1) on the real momentum axis.

We use the spline function method introduced in Ref. 18. The procedure is to expand all amplitudes X ,

$$X(p, p_0) = \sum_i S(i, p) X(p_i, p_0), \quad (3.2)$$

where $S(i, p)$ is the modified spline function of Ref. 20. Substituting Eq. (3.2) into Eq. (3.1), we obtain

$$X_{N\Delta, NN}^{JP}(p_i, p_0) = T_{N\Delta, NN}^{JP}(p_i, p_0) + \sum_j [K_{N\Delta, N\Delta}^{JP}(p_i, p_j) X_{N\Delta, NN}^{JP}(p_j, p_0) + K_{N\Delta, \pi d}^{JP}(p_i, p_j) X_{\pi d, NN}^{JP}(p_j, p_0)], \quad (3.3a)$$

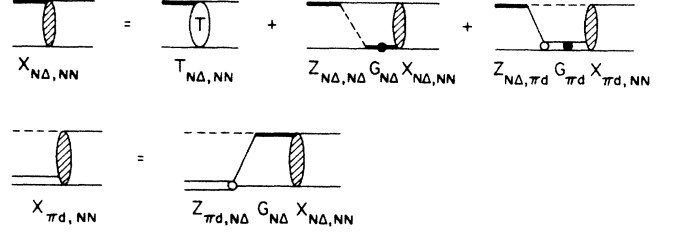


FIG. 2. Graphical representation of the Faddeev-AGS equation (2.12).

$$\Omega_{N\Delta}^{(-)+}(E) = 1 + \Omega_{N\Delta}^{(-)+}(E) [Z_{N\Delta, N\Delta}(E) + \hat{v}_{N\Delta, N\Delta}(E)] G_{N\Delta}(E), \quad (2.14a)$$

$$\Omega_{\pi d}^{(-)+}(E) = Z_{\pi d, N\Delta}(E) G_{N\Delta}(E) \Omega_{N\Delta}^{(-)+}(E), \quad (2.14b)$$

with

$$\hat{v}_{N\Delta, N\Delta}(E) = Z_{N\Delta, \pi d}(E) G_{\pi d}(E) Z_{\pi d, N\Delta}(E).$$

The above equations show how the bare interaction $V_{N\Delta, NN}$ is shadowed by the initial NN and final $N\Delta + \pi NN$ scattering. In the actual calculation, we solve Eq. (2.12) and obtain the production amplitude $T_{\pi NN, NN}$ by use of Eq. (2.10).

III. NUMERICAL METHOD

To carry out numerical calculations, it is necessary to perform standard partial-wave decompositions of all πNN scattering equations in momentum space. The needed angular momentum algebra is similar to what has been developed in the coupled-channel NN study^{7,9} and the Faddeev-AGS πd study.⁸

Our main task is to solve the integral equation (2.12) which takes the following form in the partial-wave representation:

$$X_{\pi d, NN}^{JP}(p_j, p_0) = \sum_k K_{\pi d, N\Delta}^{JP}(p_j, p_k) X_{N\Delta, NN}^{JP}(p_k, p_0), \quad (3.3b)$$

where

$$K_{\alpha\beta}^{JP}(p_i, p_j) = \int p'^2 dp' Z_{\alpha\beta}(p_i, p') G_{\beta}(p') S(j, p'). \quad (3.3c)$$

The kernel defined by Eq. (3.3c) is now finite for all real values of the relative momentum p since the logarithmic singularity of the Z 's has been integrated out. Of course, it is necessary to carry out this integration with a large number of mesh points. This has been discussed in Ref. 18. The matrix elements of the driving term $T_{N\Delta, NN}$ are finite for all real momenta and can be easily generated from our existing coupled-channel program developed in the NN study of Refs. 7 and 9.

Equations (3.3) can be solved by the standard matrix method. Care must be taken in the region where $X_{\pi d, NN}$ has a square-root branch point at the deuteron breakup threshold. This is illustrated in the lower part of Fig. 3. Clearly, we need to distribute a sufficient number of mesh points to represent this behavior at $P=311$ MeV/c. A careful test of our method has been discussed in Ref. 18. In the upper part of the same figure we also show the

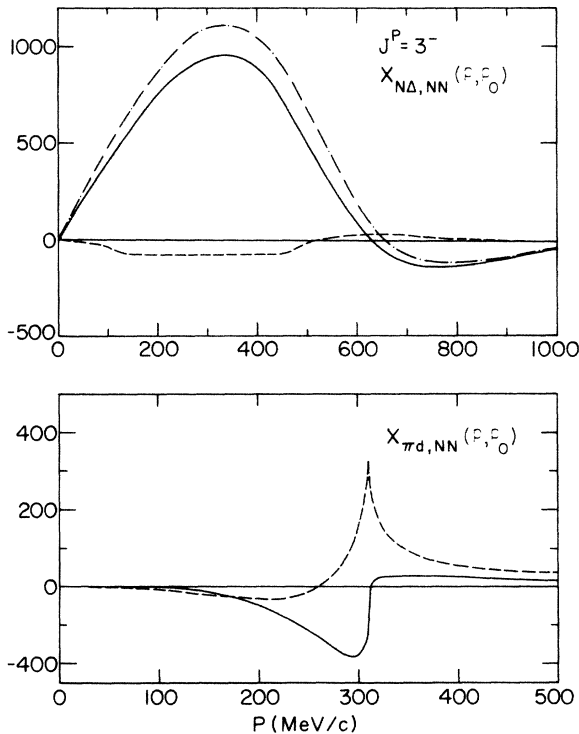


FIG. 3. The Faddeev-AGS amplitudes $X_{N\Delta, NN}$ ($L_\Delta=1, P; L_N=3, P_0$) and $X_{\pi d, NN}$ ($L_\pi=2, P; L_N=3, P_0$) of the 3^- channel calculated from Eq. (2.12). Real and imaginary parts are shown by the solid and dashed lines, respectively. Amplitudes are dimensionless. In $X_{\pi d, NN}$, the NN-FSI threshold (where NN relative energy is zero) is $P_{th}=311$ MeV/c. The impulse amplitude $V_{N\Delta, NN}$ (which has only a real part) is also shown by the dotted-dashed line in the upper graph.

$N\Delta \leftrightarrow NN$ amplitude which is smooth everywhere because of the p -wave nature of the $\Delta \leftrightarrow \pi N$ interaction.

The πNN final state interaction is treated rigorously by using the AGS amplitude $X_{\pi d, NN}$ in the calculation of the second term of Eq. (2.10). Although our method is undoubtedly much more rigorous than the phenomenological parametrization employed by Verwest¹⁶ and Dubach *et al.*,¹⁴ one must be aware of its limitation. This is due to the necessity of using a separable interaction equation (2.6) to obtain a numerically tractable AGS equation. Therefore, the calculation becomes unrealistic in the kinematic region where the final NN t matrix is far off shell. We therefore limit our FSI calculation to the region near the final state peak. In this region the energy of the relative motion of the outgoing NN subsystem is low, roughly less than 30 MeV for cases considered in this work. It is therefore sufficient to include only the $^3S_1 + ^3D_1$ and 1S_0 NN channels in defining the quasiparticle state "d." The needed separable representations of NN interactions in these two channels are taken from Ref. 21. The effect due to $^3S_1 + ^3D_1$ interaction is included exactly in solving the coupled Faddeev-AGS equation (2.12). To save computation time, the effect due to 1S_0 is treated by the perturbation

$$X_{\pi d', NN}(E) = Z_{\pi d', N\Delta}(E) G_{N\Delta}(E) X_{N\Delta, NN}(E), \quad (3.4)$$

where d' denotes the 1S_0 quasiparticle and $X_{N\Delta, NN}$ is the solution of Eq. (2.12). This is reasonable since as we will show later that the effect due to 1S_0 is much weaker.

IV. RESULTS AND DISCUSSIONS

Our main interest in this paper is to establish the extent to which our approach is valid. It is therefore sufficient to compare our theoretical predictions with the data of $pp \rightarrow \pi n \pi^+$ at 800 MeV, which is a typical example in the resonance energy region. A detailed analysis of all existing data will be presented in a later publication²² in which the nonresonant pion production mechanisms will be considered in order to account for data at lower energies.

The only adjustable parameter of the considered meson-exchange model is the cutoff parameter of the $NN \leftrightarrow N\Delta$ potential $V_{NN, N\Delta}$ which not only enters into Eqs. (2.1) and (2.2) in directly determining the production amplitude, but also plays a crucial role in elastic scattering calculation $T_{NN, NN}$ by Eq. (2.3). As mentioned in the Introduction, it is in the NN calculation of Refs. 7 and 9 that the cutoff parameter $\Lambda=650$ MeV/c is determined. The present calculation is just a prediction of our model. This must be noted in comparing our results with that of the "fit" achieved by using the lowest-order Feynman diagram.¹⁶

The most important feature of our approach is that we account for the baryon-baryon interaction by generating the $N\Delta \leftrightarrow NN$ transition $T_{N\Delta, NN}$ of Eq. (2.12) from the coupled-channel model of Refs. 7 and 9. Since the model is constructed starting from the Paris potential, the calculated $T_{N\Delta, NN}$ clearly contains mechanisms other than the conventional long-range one-pion exchange. It can be seen from Eqs. (2.2) and (2.3) that the transition is determined not only by the transition potential $V_{N\Delta, NN}$ defined

as the sum of π and ρ exchange in our model, but also by the NN scattering operator $\Omega_{NN}^{(+)}$. This important baryon-baryon dynamics is illustrated in Fig. 4, in which the half-off-shell matrix elements of $V_{N\Delta, NN}$ and $T_{N\Delta, NN}$ are compared. It is seen that the initial NN distortion effect plays an important role in the most relevant $N\Delta$ momentum region, $p \lesssim 700$ MeV/c. Its effects become negligible only for the very peripheral partial waves with $l \geq 4$. From the definition Eq. (2.3), it is clear that the differences between the solid curves and the dashed-dotted curves in Fig. 4 are quantitatively related to the accuracy of the employed πNN model in describing the corresponding NN elastic scattering. Since our model was constructed to give a good description of the NN phase shifts up to 1 GeV, our calculation of the driving term $T_{N\Delta, NN}$ of Eq. (2.12) is well defined dynamically. This strong constraint from elastic scattering is, of course, the nature of a unitary approach to πNN dynamics. It is not treated rigorously in the calculation by Betz¹² and by Dubach *et al.*^{13,14}

The coincidence differential cross section of $pp \rightarrow pn\pi^+$ can be written as

$$\frac{d^3\sigma}{dp d\Omega_p d\Omega_\pi} = K \left| \sum_{J,P,\alpha,\beta} T_{\alpha,\beta}^{JP} \right|^2, \quad (4.1)$$

where K is a kinematic factor, p is the outgoing proton momentum, Ω_p and Ω_π are, respectively, the angles of the detected proton, and π^+ , α , and β are the orbital-spin-isospin quantum numbers needed to specify the initial pp and final π^+pn partial waves in the channel of total angular momentum J and parity P . The dynamical features of the production mechanism can be seen by examining how the cross section is built up from summing the partial wave contributions in Eq. (4.1). Let us first examine the direct Δ production mechanism [Fig. 1(a)] calculated by keeping only the first term of Eq. (2.10). In column 3 of Table I we show the contribution from each partial wave. The large contributions are from $1 \leq l \leq 5$ partial waves. The suppression of $J=0$ partial waves is, of course, partially due to the large distortion effect illustrated in Fig. 4, but is mainly due to the geometric factors dictating the $NN \rightarrow N\Delta \rightarrow NN\pi$ transition. This finding is consistent with the NN phase shift analysis in which the inelasticity of 1S_0 is extremely small. The largest term comes from peripheral partial waves, 3^- (the initial NN state is 3F_3) for this particular kinematics. In the OPE model of Kloet and Silbar similar suppression of low partial waves is also noted.

In the last column of Table I, we see that as the maximum value of JP in the sum of partial-wave contributions is increased, the cross section is also increased. Clearly, all partial waves contribute coherently. Hence the summed cross section is sensitive to the small part of the amplitude. Although the individual contributions of $2 \leq l$ partial waves are small, as seen in the third column, an accurate calculation of these low l amplitudes is important in any attempt of using the production data to examine the πNN dynamics. For the same reason it is necessary to calculate up to very high partial waves so that the coherence can be fully included.

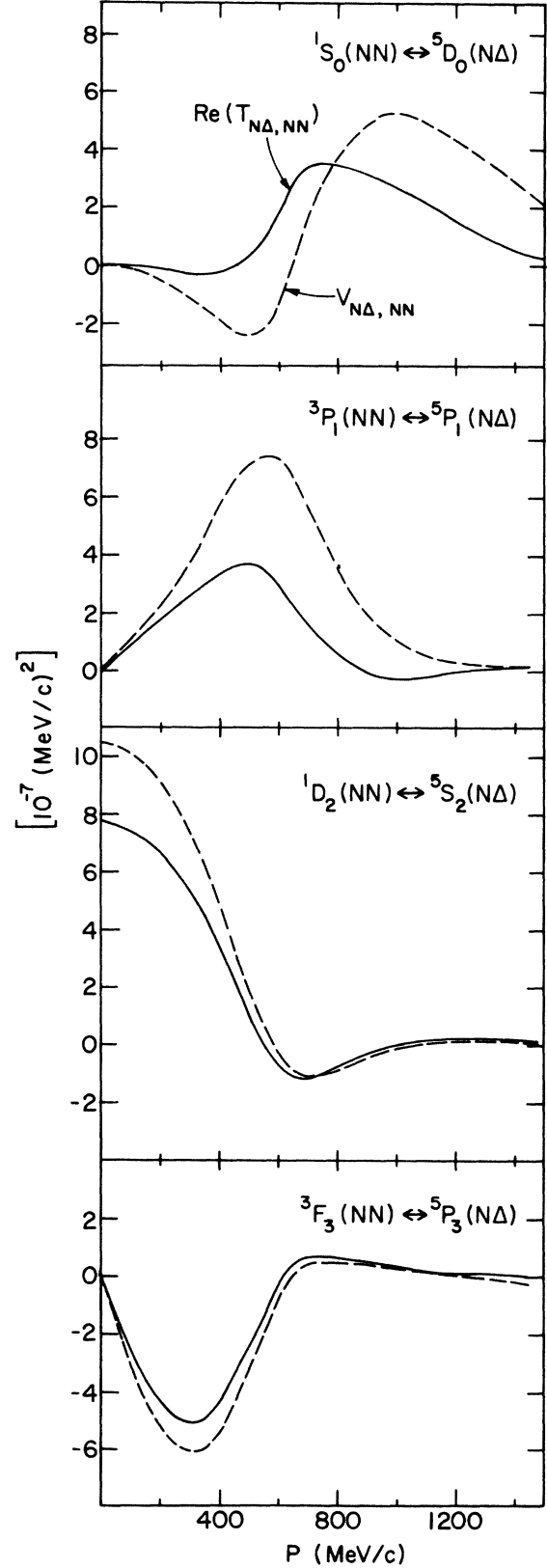


FIG. 4. Comparison of the matrix elements of $T_{N\Delta, NN}(p, p_0)$ calculated from solving Eqs. (2.2) and (2.3) and the $N\Delta \rightarrow NN$ transition potential $V_{N\Delta, NN}(p, p_0)$, where $p_0 = 300$ MeV/c. For the channels with $l(NN) \geq 4$, the difference becomes negligible and hence is not presented.

TABLE I. Partial wave contributions to the unpolarized differential cross section of $pp \rightarrow p\pi\pi^+$ at 800 MeV with the outgoing proton momentum $P=1000$ MeV/c, $\theta_p=14.5^\circ$, and $\theta_\pi=42^\circ$; α and β denote orbital-spin-isospin quantum numbers needed to specify the initial pp and final $p\pi\pi^+$ states. The third column is the contribution from each partial wave. The results from the coherent sum of partial waves up to $A=J^P$ are in column 4.

J^P	Initial NN state	$\left. \frac{d^3\sigma}{dp d\Omega_p d\Omega_\pi} \right $	
		$K \left \sum_{\alpha\beta} T_{\alpha\beta}^{J^P} \right ^2$	$K \left \sum_{A \leq J^P} T_{\alpha\beta}^A \right ^2$
0^-	3P_0	0.076	0.076
0^+	1S_0	0.003	0.080
1^-	3P_1	0.316	0.396
2^-	$^3P_2 + ^3F_2$	0.861	1.636
2^+	1D_2	0.341	1.981
3^-	3F_3	2.730	4.426
4^-	$^3F_4 + ^3H_4$	0.132	5.882
4^+	1G_4	0.942	7.948
5^-	3H_5	0.983	12.47
6^-	$^3H_6 + ^3J_6$	0.013	13.11
6^+	1I_6	0.084	14.06
7^-	3J_7	0.081	15.51
8^-	$^3J_8 + ^3L_8$	0.002	15.70
8^+	1K_8	0.010	16.04

The simplest pion production mechanism is due to the impulse mechanism in which the initial NN and final π NN distortions are absent. The impulse calculation corresponds to setting the distortion factors $\Omega_{NN}^{(+)} = \Omega_{N\Delta}^{(-)+} = 1$ in Eq. (2.13). It is of interest to see in which way the dynamical features of the bare production mechanism become hidden by the distortion effects. It is seen in the lower part of Fig. 5 that the distortion can reduce the magnitude of the cross section by about 30% for this particular kinematics. Part of this reduction is, of course, due to the initial NN distortion shown in Fig. 4. Further reduction comes from the interaction due to the one-pion exchange $Z_{N\Delta, N\Delta}$ and nucleon exchange $Z_{\pi d, N\Delta}$, as described in Eq. (2.14).

We found that the reduction of the magnitude of the cross section is mainly due to the initial NN distortion. This is shown in Table II, and when the NN distortion is neglected by setting $\Omega_{NN}^{(+)}$ of Eq. (2.2) to 1, the magnitude of the cross section is increased. In the last column of the same table we show the results calculated by further setting $Z_{\pi d, N\Delta} = 0$. By comparing these two results, it is clear that the distortion due to NN interaction in the presence of a spectator pion, characterized by the quasiparticle interaction v_d , has very little effect. Its main effect is in the FSI region, which will be discussed later.

The most dramatic effect due to distortions is in the polarization. As is seen in the upper part of Fig. 5, the impulse term gives a very small analyzing power A_y , while the result from the full calculation is significant for all momentum and changes sign at $p \cong 900$ MeV/c. Our result suggests that any attempt to use the polarization data

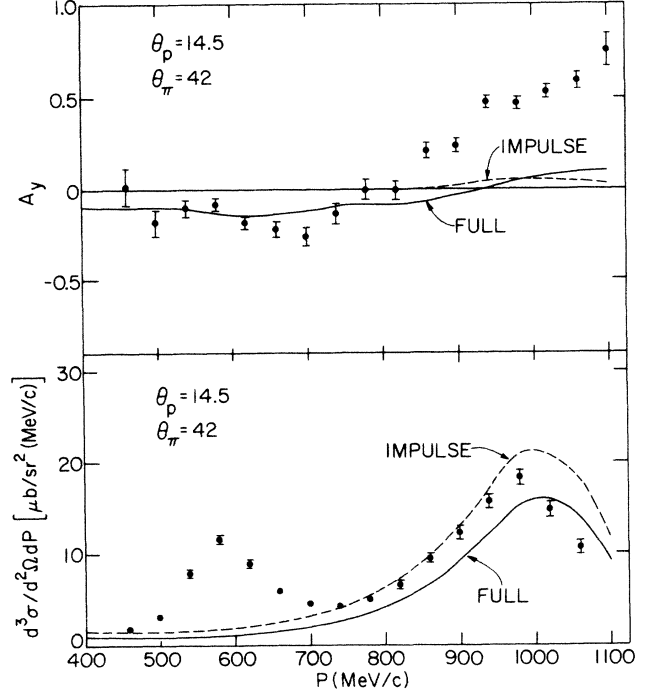


FIG. 5. Comparison of the full calculation (—) with the impulse approximation result (---) for $pp \rightarrow p\pi\pi^+$ at 800 MeV. Only the direct Δ -production term is included in this calculation. The data are from Ref. 2.

to search for any unconventional baryon-baryon interaction, such as the formation of a six-quark state, must be carried out with a careful account of the distortion effects.

We now turn to investigating the kinematical region which is dominated by the final state interaction, i.e., the second term of Eq. (2.10). This is the low momentum region $p < 700$ MeV/c in Fig. 5. The kinetic energy of the relative motion of the outgoing np pair in this region is roughly less than 30 MeV. Hence it is sufficient to consider the np interaction in only the $^3S_1 + ^3D_1$ and 1S_0 channels. The $^3S_1 + ^3D_1$ interaction is treated to all orders by solving the coupled quasiparticle equation (2.12). The 1S_0 channel is only treated perturbatively using Eq. (3.4). This is justified since the 1S_0 channel is suppressed geometrically; it contributes to the $J^P = 0^-, 2^-, 4^-, \dots$ channels, which couple weakly to the intermediate $N\Delta$ state. The weakness of the 1S_0 FSI has also been pointed out by Dubach *et al.*¹⁴ and is verified in our calculation shown in Fig. 6.

In Table III we show the partial wave contributions to the cross section in the FSI region. The first column is the small contribution from the direct Δ production term which converges very quickly at $J=4$ instead of $J=8$ in the high momentum Δ region (see Table I). When the FSI term is included, the calculated cross section increases to a value close to the data. The coherence is destructive when the maximum value of J^P in the sum of Eq. (4.1) is increased from 4^- to 5^- . This delicate result comes out from solving the coupled Faddeev-AGS equation (2.12) in each partial wave. The FSI interaction depends strongly

TABLE II. Same as Table I. $\Omega_{NN}^{(+)}$ is the initial NN distortion operator defined by Eq. (2.2). $Z_{\pi d, N\Delta}$ is the nucleon-exchange interaction due to the decay of the quasiparticle d defined by the separable representation of Eq. (2.6).

J^P	$\left[\frac{d^3\sigma}{dp d\Omega_p d\Omega_\pi} \right] = K \left \sum_{\substack{A \leq J^P \\ \alpha\beta}} T_{\alpha\beta}^A \right ^2$		
	Exact	$\Omega_{NN}^{(+)}=1$	$\Omega_{NN}^{(+)}=1, Z_{\pi d, N\Delta}=0$
0 ⁻	0.076	0.079	0.079
0 ⁺	0.080	0.091	0.098
1 ⁻	0.396	0.394	0.390
2 ⁻	1.636	2.558	2.568
2 ⁺	1.981	3.155	3.201
3 ⁻	4.426	6.871	7.191
4 ⁻	5.882	8.730	9.080
4 ⁺	7.948	11.27	11.70
5 ⁻	12.47	16.54	17.06
6 ⁻	13.11	17.28	17.82
6 ⁺	14.06	18.34	18.91
7 ⁻	15.51	19.92	20.50
8 ⁻	15.70	20.15	20.74
8 ⁺	16.04	20.52	21.12

TABLE III. Same as Table I, except at outgoing proton momentum $P=600$ MeV/c. Δ is the result calculated from keeping only the direct Δ production [first term of Eq. (2.10)]; Δ +FSI is the full calculation including also the ${}^3S_1+{}^3D_1$ final state interaction (FSI) term.

J^P	$\left[\frac{d^3\sigma}{dp d\Omega_p d\Omega_\pi} \right] = K \left \sum_{\substack{A < J^P \\ \alpha\beta}} T_{\alpha\beta}^A \right ^2$	
	Δ	Δ +FSI
0 ⁻	0.012	0.012
0 ⁺	0.013	0.020
1 ⁻	0.156	0.932
2 ⁻	0.162	1.002
2 ⁺	0.785	5.211
3 ⁻	1.402	8.681
4 ⁻	1.397	8.634
4 ⁺	1.177	7.349
5 ⁻	1.110	6.954
6 ⁻	1.110	6.957
6 ⁺	1.114	6.988
7 ⁻	1.114	6.996
8 ⁻	1.114	6.996
8 ⁺	1.115	6.996

on the eigenchannel partial wave, and cannot be realistically represented by a common factor for all partial waves, as is usually done in a phenomenological parametrization of FSI. Our approach is the necessary consistent procedure within our formulation, and is clearly dynamically well defined.

With the above theoretical understanding of the structure of our approach, we now compare our full calculations with the data at 800 MeV. We first note here that the total pion production amplitude has two components. The first one is due to the kinematics that the detected proton is from the decay of $\Delta^{++} \rightarrow p\pi^+$. The weaker amplitude is due to $\Delta^+ \rightarrow n\pi^+$ in the presence of a spectator proton. In Fig. 7 we show their relative importance. Clearly, the amplitude due to $\Delta^+ \rightarrow n\pi^+$ is much weaker, but its effect must also be included in order to properly interpret the data.

Our results at 800 MeV are compared with the data² in

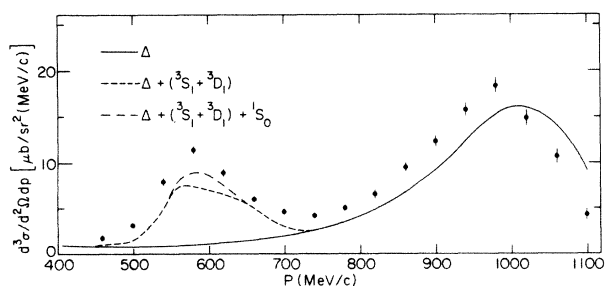


FIG. 6. Same reaction as Fig. 5. The solid curve denotes the results calculated from keeping only the direct Δ -production term. The dashed (dashed-dotted) curve is the full calculation including ${}^3S_1+{}^3D_1$ (${}^3S_1+{}^3D_1$ and 1S_0) in defining the NN quasiparticle state d .

Fig. 8. The solid curves are the results calculated from keeping only the direct Δ production term [Fig. 1(a)]. The dashed curves include the contribution from the FSI term [Fig. 1(b)]. It is seen that both the shapes and the magnitudes of the differential cross sections are reasonably reproduced in the Δ excitation region. The discrepancies in the high momentum Δ region could indicate the deficiency of the $\pi+\rho$ exchange parametrization of the $N\Delta \rightarrow NN$ transition since the corresponding $N\Delta$ momentum is large and the cross sections become sensitive to the short-range part of the baryon-baryon interaction.

The calculations in the FSI region are also reasonable. Both the shapes and the peak positions are well reproduced. At $\theta_p=14.5^\circ$ and $\theta_\pi=21^\circ$, the theory is in good agreement with the data. In other kinematic regions, the calculated FSI peaks are lower than the data. We must note here that our results are not renormalized in any way

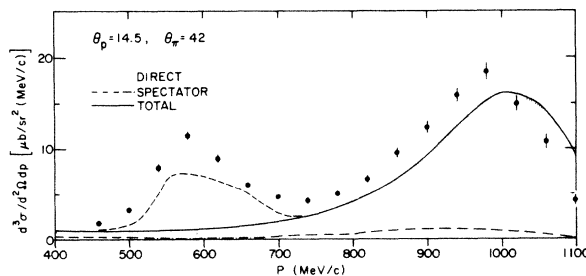


FIG. 7. Same reaction as Fig. 5. The dotted curve is direct Δ -production followed by the $\Delta^{++} \rightarrow p\pi^+$ decay. The dashed-dotted curve is the direct Δ production due to $\Delta^+ \rightarrow n\pi^+$ in the presence of a spectator proton. The solid curve is the coherent sum of both mechanisms. The dashed curve includes the FSI term.

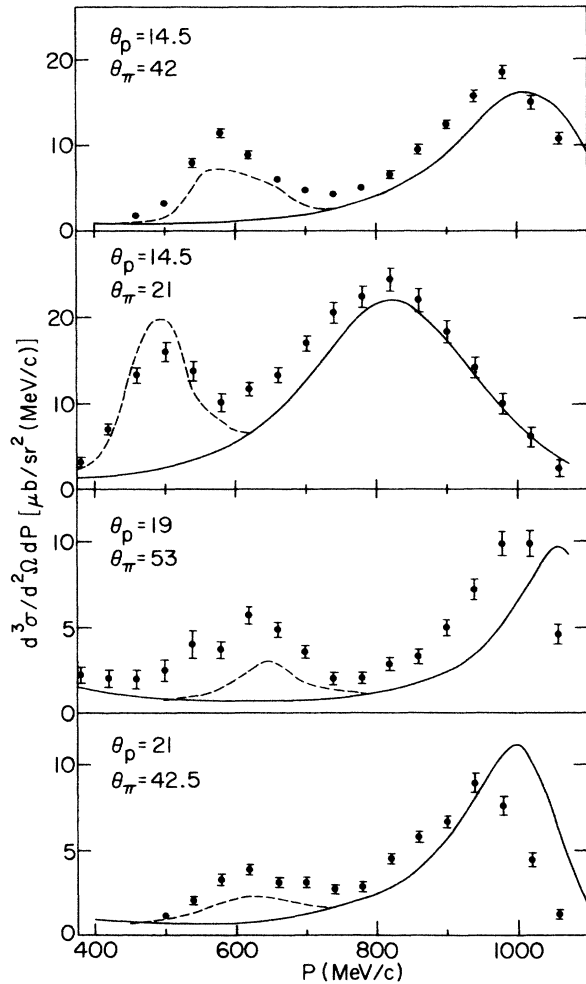


FIG. 8. Comparison of our calculation of $pp \rightarrow pn\pi^+$ with the data (Ref. 2) at 800 MeV. The solid curves are the results calculated from keeping only the direct Δ -production term. The dashed curves include the FSI contribution due to ${}^3S_1 + {}^3D_1$ interactions.

from the values obtained from our unitary calculation. FSI calculations of Ref. 14 involve an adjustable parameter in fitting the data.

In Fig. 9 we show two typical results for the analyzing power A_y , calculated by keeping only the direct Δ production term. We have also investigated the effect of FSI on A_y . No improvement has been found. The difficulty of the meson theory in describing the polarization data has already been found in NN elastic scattering.^{7,9} The results shown in Fig. 9 are therefore just more evidence of the same dynamical problem which could require a solution from quark physics.

To end this section, we want to discuss the relationship between our approach and the unitary approach^{13,14} based on the one-pion-exchange model. It is expected that the OPE model is dynamically insufficient for describing all π NN processes. For instance, the unitary calculation of Kloet and Silbar¹⁵ has little success in describing NN elastic scattering and various gross properties of NN total cross sections. Despite this obvious dynamical deficiency, the OPE unitary calculation of Ref. 14 can describe the

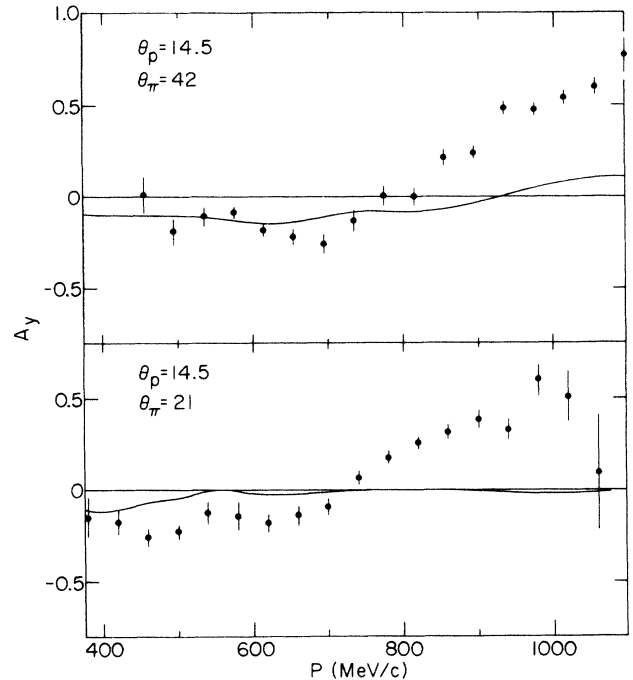


FIG. 9. Comparison of our calculation of the analyzing power A_y for $pp \rightarrow pn\pi^+$ with the data at 800 MeV. Only the direct Δ -production term is kept in the calculation.

pion production cross section as well as the present, much more consistent, approach in the region dominated by the Δ excitation (but not in the FSI region). To understand this somewhat puzzling situation, we examine the properties of our approach in the limit that only one-pion-exchange dynamics is kept. The OPE model can be obtained in our formulation by (a) replacing the Paris potential in the NN calculation [Eq. (2.3)] by the standard one-pion-exchange potential, (b) setting the $\pi d \leftrightarrow N\Delta$ driving term $Z_{\pi d, N\Delta}$ to zero in solving Eq. (2.12) so that no NN interaction in any π NN intermediate state is allowed, and (c) keeping only the one-pion-exchange part of the $V_{NN \leftrightarrow N\Delta}$ potential. Our OPE model is, of course, not quantitatively identical to that of Ref. 15, because of the differences in formulating the unitary π NN scattering theory. It is, however, sufficient for our present discussion about the importance of π NN dynamics other than the long-range one-pion exchange.

The accuracy of the OPE model in pion production calculations can be qualitatively estimated by examining the results shown in Fig. 10 and Table II. We have seen in Table II that the effect due to the quasiparticle interaction $Z_{\pi d, N\Delta}$ is very small. This indicates that the NN interaction in the π NN intermediate state, which is not present in the OPE model, can be safely neglected. Hence, the main difference between our approach and the OPE model is in the treatment of initial NN distortion. This difference is shown in Fig. 10, in which we compare the half-off-shell matrix elements of $T_{N\Delta, NN}$ calculated from our full model and the OPE model. We see that two matrix elements are very different for $l \leq 2$ partial waves, but are very close for all $l \geq 3$ peripheral partial waves. This

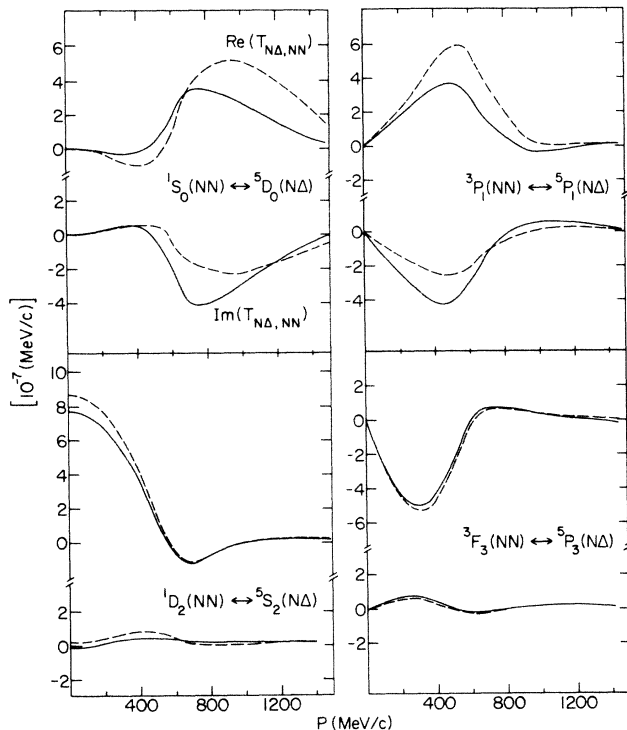


FIG. 10. Comparison of the matrix elements of the $NN \rightarrow N\Delta$ transition calculated from the model equation (1.1) (solid curve) and the OPE model (dashed curve) described in the text.

means that the important distortion effects (see Table II) for the peripheral partial waves, which are the main source of pion production (see Table I), can be appropriately accounted for by the OPE unitary calculation. This explains why although the unitary OPE model is not adequate for describing NN elastic scattering, it nevertheless can account for pion production if the parameters of the model are properly determined from πN scattering.

V. SUMMARY

Starting with the model Hamiltonian equation (1.1), we have followed the πNN unitary formulation of Ref. 6 to derive a set of scattering equations for the study of $NN \rightarrow NN\pi$ reaction. The calculation consists of two major steps. First, we need to solve the baryon-baryon

scattering equations (2.2) and (2.3). This coupled-channel calculation simultaneously generates the NN elastic scattering amplitude $T_{NN, NN}$ and the $NN \rightarrow N\Delta$ transition matrix $T_{N\Delta, NN}$. The next step is to use $T_{N\Delta, NN}$ as the driving term to solve the Faddeev-AGS scattering equation (2.12). Its solution is used to calculate the production amplitude equation (2.10). We have presented a practical numerical procedure of using the newly developed spline-function method to solve the considered Faddeev-AGS equation.

We have shown that the pion production cross section is dominated by the peripheral partial waves. However, because of the coherent interference between partial wave contributions (see Table I), a quantitative test of theory also needs an accurate calculation of small amplitude due to $l \leq 2$ channels.

We have shown that the initial NN and final πNN distortions play an important role in determining the $NN \rightarrow NN\pi$ cross section. Our coupled-channel treatment of the NN initial distortion [Eqs. (2.2) and (2.3)] is essential for a correct prediction of the magnitude of the production cross section in the Δ -excitation region. This has been understood by showing the close relationship between the initial NN distortion effect and our previous NN elastic scattering calculation,^{7,9} which has given a good description of NN phase shifts. We have also shown that a Faddeev-AGS treatment of the final πNN distortion is essential for a quantitative understanding of the FSI peaks of the $NN \rightarrow NN\pi$ cross sections.

Our results for $pp \rightarrow pn\pi^+$ at 800 MeV are only in qualitative agreement with the data. The discrepancies between our predictions and the data are due to the intrinsic deficiencies of the starting meson-exchange Hamiltonian equation (1.1). The present result has provided further evidence that the πNN dynamics cannot be described completely by the conventional meson-exchange model. Of course, this conclusion must be carefully checked by investigating the mesonic effects neglected in this calculation, such as the effect due to nonresonant πN interaction. This has been addressed in Ref. 9 for NN and πd elastic scattering, and will be presented in Ref. 22 for the $NN \rightarrow NN\pi$ reaction.

This work was supported by the U.S. Department of Energy, Nuclear Physics Division, under Contract No. W-31-109-ENG-38.

*Present address: Department of Physics, Faculty of Liberal Arts, Shizuoka University, Shizuoka, Japan.

¹J. Hudomalj-Gabitzsch *et al.*, Phys. Rev. C **18**, 2666 (1978).

²A. D. Hancock *et al.*, Phys. Rev. C **27**, 2742 (1983).

³C. E. Waltham *et al.*, Nucl. Phys. **A433**, 649 (1985).

⁴C. L. Hollas *et al.*, Phys. Rev. Lett. **55**, 29 (1985).

⁵G. Glass *et al.*, Phys. Lett. **127**, 27 (1983).

⁶T.-S. H. Lee and A. Matsuyama, Phys. Rev. C **32**, 516 (1985).

⁷T.-S. H. Lee, Phys. Rev. Lett. **50**, 157 (1983); Phys. Rev. C **29**, 195 (1984).

⁸A. S. Rinat and A. W. Thomas, Nucl. Phys. **A282**, 365 (1977); A. S. Rinat, E. Hammel, Y. Starkand, and A. W. Thomas, *ibid.* **A329**, 285 (1979); N. Giraud, C. Fayard, and G. H.

Lamot, Phys. Rev. C **21**, 1959 (1980); C. Fayard, G. H. Lamot, and T. Mizutani, Phys. Rev. Lett. **45**, 524 (1980), A. Matsuyama and K. Yazaki, Nucl. Phys. **A364**, 477 (1981).

⁹T.-S. H. Lee and A. Matsuyama, Phys. Rev. C **32**, 1986 (1985); Argonne National Laboratory Report No. PHY-4863-TH-86, 1986.

¹⁰M. Lacombe, B. Loiseau, J. M. Richard, R. Vinh Mau, J. Cote, P. Pine, and K. Turreil, Phys. Rev. C **21**, 861 (1980).

¹¹The meaning of ρ exchange is lost when $\Lambda = 650$ MeV is used. It is more appropriate to consider ρ exchange as just a phenomenological device which leads to a good fit to the data.

¹²The calculation by M. Betz is in an invited paper presented at the Workshop on Pion Production and Absorption in Nuclei,

- Bloomington, Indiana, Oct. 22–24, 1981 (TRIUMF Report No. TRI-81-59, 1981).
- ¹³J. Dubach, W. M. Kloet, A. Cass, and R. R. Silbar, *Phys. Lett.* **106B**, 29 (1981).
- ¹⁴J. Dubach, W. M. Kloet, and R. R. Silbar, *J. Phys. G* **8**, 475 (1982); *Phys. Rev. C* **33**, 373 (1986).
- ¹⁵W. M. Kloet and R. R. Silbar, *Nucl. Phys.* **A338**, 281 (1980); **A338**, 317 (1980); **A364**, 346 (1981).
- ¹⁶B. J. Verwest, *Phys. Lett.* **83B**, 161 (1979); E. A. Umland, I. M. Duck, and G. S. Mutchler, Rice University report, 1980.
- ¹⁷See review articles collected in *Modern Three-Hadron Physics*, edited by A. W. Thomas (Springer, Heidelberg, 1977).
- ¹⁸A. Matsuyama, *Phys. Lett.* **152B**, 42 (1985).
- ¹⁹J. H. Hetherington and L. H. Schick, *Phys. Rev.* **137**, B935 (1965); R. Aaron and R. D. Amado, *ibid.* **150**, 857 (1966).
- ²⁰W. Glöckle, G. Hasberg, and A. R. Neghabian, *Z. Phys. A* **305**, 217 (1982).
- ²¹N. Giraud, C. Fayard, and G. H. Lamot, *Phys. Rev. C* **21**, 1959 (1980).
- ²²A. Matsuyama (unpublished).